



Oscillon Dynamics and Rogue Wave Generation in Faraday Surface Ripples

H. Xia,^{*} T. Maimbourg,[†] H. Punzmann, and M. Shats

Research School of Physics and Engineering, The Australian National University, Canberra ACT 0200, Australia
(Received 13 July 2012; published 14 September 2012)

We report new experimental results which suggest that the generation of extreme wave events in the Faraday surface ripples is related to the increase in the horizontal mobility of oscillating solitons (oscillons). The analysis of the oscillon trajectories in a horizontal plane shows that at higher vertical acceleration, oscillons move chaotically, merge and form enclosed areas on the water surface. The probability of the formation of such craters, which precede large wave events, increases with the increase in horizontal mobility.

DOI: [10.1103/PhysRevLett.109.114502](https://doi.org/10.1103/PhysRevLett.109.114502)

PACS numbers: 47.35.Pq, 47.27.Cn, 47.52.+j

Perturbations of the interface between two fluids (for example, water and air) subjected to vertical vibration have been studied for several hundred years, producing a wealth of physics on pattern formation [1–4], turbulence [5], wave turbulence (e.g., [6–8]), instabilities and solitons [9–13], physics of bouncing orbiting droplets (walkers) [14], extreme wave events, or rogue waves [15], and others. This object, whose systematic studies have been pioneered by Faraday [16], still remains not fully understood. Moreover, new experimental capabilities reveal an even richer spectrum of effects in Faraday surface ripples.

Parametrically excited ripples are observed as ordered states, or patterns (usually in dissipative fluids), and as disordered states (at lower dissipation and/or higher drive), often referred to as turbulence. In highly dissipative fluids, such as a granular gas [2], a regular pattern is described as a discrete lattice of harmonically coupled elements, or oscillons [17]. Recently, we have proposed [13] that at low dissipation, Faraday ripples also represent ensembles of oscillons and that the order-to-disorder transition can be due to a change in the oscillons' horizontal mobility. Such a mobility, which had not been confirmed experimentally, may be responsible for the broadening of the frequency spectra [7,11,18]. It is also possible that the increase in the oscillon mobility is related to the generation of large wave events previously reported in the Faraday wave experiment [15].

In this Letter we report the first measurements of the oscillon horizontal mobility in a low dissipation fluid, water. It is shown that transitions from ordered lattice of oscillons to a disordered state occur gradually with the increase in forcing. The oscillon mobility is correlated with spectral broadening. At low dissipation, oscillons' mobility appears to be higher than in strongly dissipative fluids, allowing random walk within a crystal and leading to the oscillon overlapping and merger. The increase in the merger rate with the increase in the drive is correlated with a strong increase in the probability of rogue waves.

Visualization of the surface ripples can be achieved by transmitting light through the fluids. The main problem here

is the refraction of light if the optical indices of the two fluids are different. Though there are ways to recover the surface elevation field from refracted light (e.g., [19,20]), they do not work when the wave steepness is high. There are two known techniques capable of avoiding this problem. The first uses colloidal suspensions of the light diffusing agent (e.g., suspended imaging particles) such that the intensity of light transmitted is inversely proportional to the local depth. The diffusing light photography technique was successfully used in the Faraday ripple studies at the air-water interface [6,21]. Another option is to use two fluids with matching refractive indices [22]. One of the fluids needs to be light absorbing. This however restricts the choice of the fluids. The latter technique has been used for spatiotemporal characterization of patterns [3] and pattern instabilities [4] at higher dissipation. In this paper we employ time-resolved diffusing light imaging technique which is more suitable for studies at the water-air interface, characterized by lower wave dissipation.

A light source is an LED panel placed underneath the transparent bottom of a circular container (200 mm diameter, 40 mm deep). The container is vibrated vertically at the frequency of 60 Hz. A diffusive agent, such as suspended imaging particles (50 μm) or a small amount (< 2% in volume) of milk is added to water. The fluid surface is filmed from above using an Andor Neo sCMOS camera (resolution 2560×2160 at 30 fps, 128×128 pix at 1100 fps). The camera can be synchronized with a particular phase of the wave amplitude. The surface elevation of the oscillon fields at time t is computed from the 2D intensity distribution $I(x, y, t)$ as

$$h(x, y, t) \sim \ln \frac{I(x, y, t)}{\langle I_b(x, y) \rangle}, \quad (1)$$

where $\langle I_b(x, y) \rangle$ is the background intensity distribution of light transmitted through unperturbed fluids.

Figure 1 shows snapshots of the surface elevation $h(x, y, t)$, phase synchronized with the maximum in the wave amplitude at 30 Hz (the first subharmonic of the forcing frequency) for two levels of the supercriticality

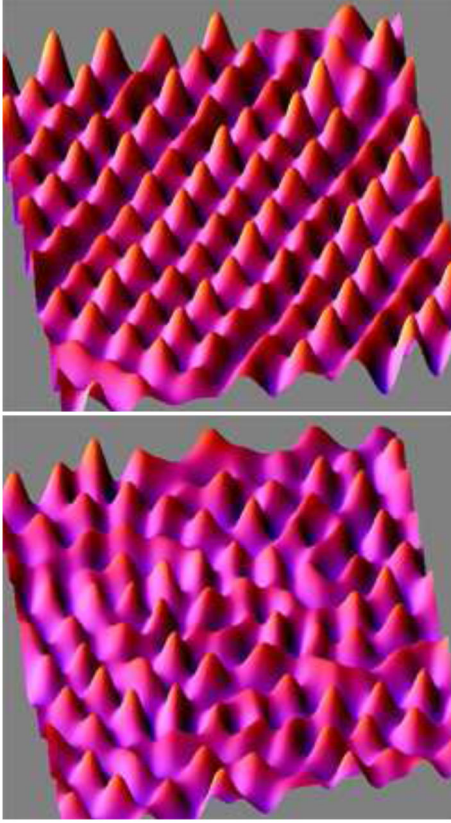


FIG. 1 (color online). Measured surface elevation snapshots derived from the diffusive light imaging analysis of the surface ripples under parametric excitations at 60 Hz (top) $\epsilon = 1.4$, and (bottom) $\epsilon = 3.8$.

$\epsilon = (A - A_{\text{th}})/A_{\text{th}}$, where A is the amplitude of the sinusoidal acceleration (in the reported experiments at the forcing frequency of 60 Hz, $0.5g < A < 3g$), and A_{th} is the threshold acceleration for the parametric generation of Faraday waves. At $\epsilon = 1.4$, Fig. 1(a), a reasonably regular square lattice of oscillons is observed, similar to those observed at higher dissipation and lower supercriticalities (typically $\epsilon < 0.5$) [3,4]. At higher forcing, at $\epsilon = 3.8$, just below the threshold of the droplet formation [Fig. 1(b)], the lattice becomes disordered, showing merger of adjacent oscillons and larger variability of the peaks amplitudes.

At low vertical acceleration, frequency spectra show narrow multiple harmonics of the main subharmonic of the excitation frequency, as seen in Fig. 2(a). At higher drive, these harmonics become substantially broadened. It has been recently found that multiple harmonics in the frequency spectra are observed even when the liquid surface is subcritical to parametric wave excitation and a single isolated oscillon is excited by external perturbation of the surface [13]. It was speculated that the observed spectral broadening [see inset in Fig. 2(a)] is caused by the Doppler broadening due to the horizontal mobility of oscillating solitons.

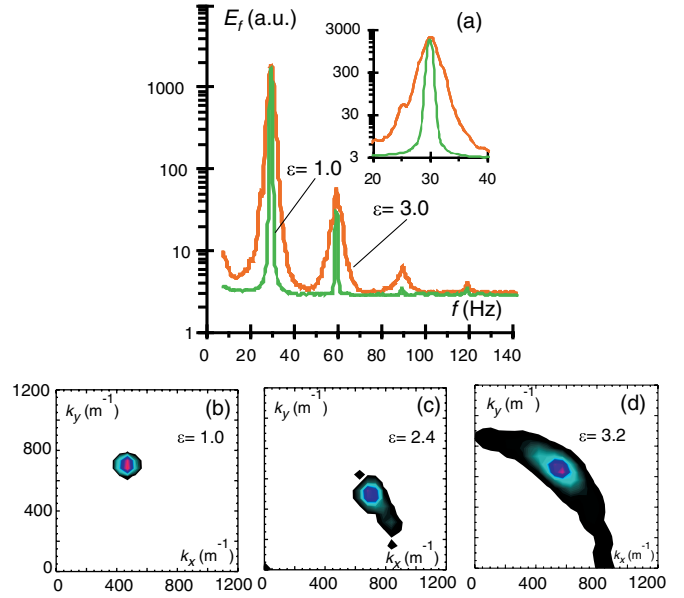


FIG. 2 (color online). (a) Frequency spectra of the surface elevation derived from the fast (750 fps) video at two supercriticality levels $\epsilon = 1.0$ and 3.0 . Inset shows zoom into the first subharmonic at 30 Hz. (b–d) The wave number spectra of the surface elevation at different excitation levels of $\epsilon = 1.0, 2.4, 3.2$.

A wave number spectrum shows one dominant peak corresponding to the lattice period, Fig. 2(b). However the onset of the crystal dislocations and relative motion of the oscillons within the lattice spread spectral energy in 2D k -spectrum over a broad range of azimuthal angles $\arctan(k_y/k_x)$, leaving however the dominant peak $k_{\perp} = (k_x^2 + k_y^2)^{1/2}$ unchanged, Figs. 2(c) and 2(d).

To study oscillon mobility, we perform tracking of the oscillon maxima in the phase synchronized movie as follows. After preprocessing a movie using ImageJ software [23], the isolines of the surface heights are analyzed to identify oscillons of various amplitudes (high and low). Then in each time frame the position, size, and circularity of oscillons are recorded. A particle tracking algorithm [24] is then applied to follow trajectories of all of the oscillons in the field of view of the camera using the nearest neighbor algorithm. A maximum distance for the nearest neighbor search is set to less than the lattice period. The noncircularity of the blobs is indicative of a merger of individual oscillons which are circular.

Figs. 3(a) and 3(b) show examples of the oscillon trajectories tracked over 10 s (300 oscillon periods) within a square lattice for two levels of supercriticalities, $\epsilon = 1.4$ and $\epsilon = 3.8$. The statistical analysis of the trajectories gives the ensemble and time averaged quantities, such as mean velocity of oscillon along the trajectory, its average excursion from the initial position, the collision rate of oscillons (mean inverse lifetime between the merger events), etc. The mean velocity of oscillons in a lattice

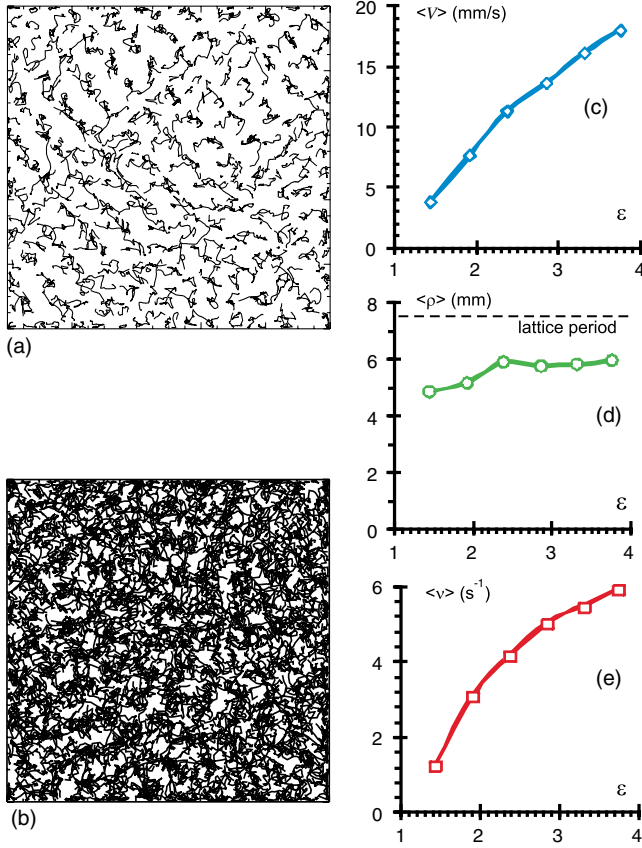


FIG. 3 (color online). Trajectories of the oscillon maxima tracked over 10 seconds within the crystal at (a) $\epsilon = 1.4$ and (b) $\epsilon = 3.8$. Statistics of the oscillon trajectories in the crystal at different supercriticalities: (c) average velocity of the oscillon excursion, (d) average oscillon orbit size (dashed line shows the lattice period), (e) average merger rate per oscillon.

increases with the increase in the drive, Fig. 3(c). The average size of a “cloud” covered by an oscillon during its drift, $\langle \rho \rangle = (1/N) \sum_{i=1}^N \sqrt{(x_{\max}^i - x_{\min}^i)^2 + (y_{\max}^i - y_{\min}^i)^2}$, where i is the oscillon label, is shown in Fig. 3(d). The oscillon excursion becomes large at rather low excitation amplitudes and it is comparable to the lattice period, $L = 2\pi/k_{\perp}$, such that the probability of the merger events increases with the increase in the average oscillon velocity. The average merger rate per oscillon per unit time is shown in Fig. 3(e).

The observed increase in spectral broadening with the increase in drive seen in Fig. 2, is correlated with the strong increase in the oscillon mobility found from the analysis of oscillon trajectories, Fig. 3. This confirms the hypothesis [13] that broadening of the frequency spectra is a sensitive function of the oscillon mobility. Similarly to the mean oscillon velocity, Fig. 3(c), spectral width of the frequency harmonics also increases proportionally to the vertical acceleration [18].

The motion of oscillons in the range of supercriticalities $\epsilon = (1-4)$ studied here, is random. A horizontal motion of

oscillons in a lattice becomes stochastic at relatively low drive. This has been studied by analyzing trajectories of the oscillon pairs. A distance between pairs of adjacent (in rows and columns) oscillons in a lattice, $\Delta\rho(t)$, has been computed for the duration of the pair’s lifetime (the shortest of the two in a pair). The autocorrelation function of $\Delta\rho(t)$ decays fast, a typical correlation time is less than 0.3 s. Transitions from order to disorder have been studied in [25], where it has been shown that the correlation length decreases strongly at rather low supercriticality ($\epsilon < 0.2$). In the reported experiments forcing is much stronger, so the motion of oscillons in a lattice is random.

As the mobility increases with drive, the probability of large wave events, or rogue waves, increases too as has been reported in [15]. By large events we mean positive short-lived (1–3 periods) surface elevations in excess of (4–5) mean square heights of the background wave field. One of such events is illustrated in Fig. 4(a). Probability density functions (PDF) are shown in Fig. 4(b). Note that the PDF is plotted versus the surface height normalized by the corresponding root-mean-square value. Probability of large events increases with the increase in the drive by several orders of magnitude.

The observed correlation of the probability of large wave events with the increase in oscillon mobility suggests a connection. However the generation of rogue waves cannot be attributed to a simple superposition of oscillons since the merger of two oscillons leads to the formation of

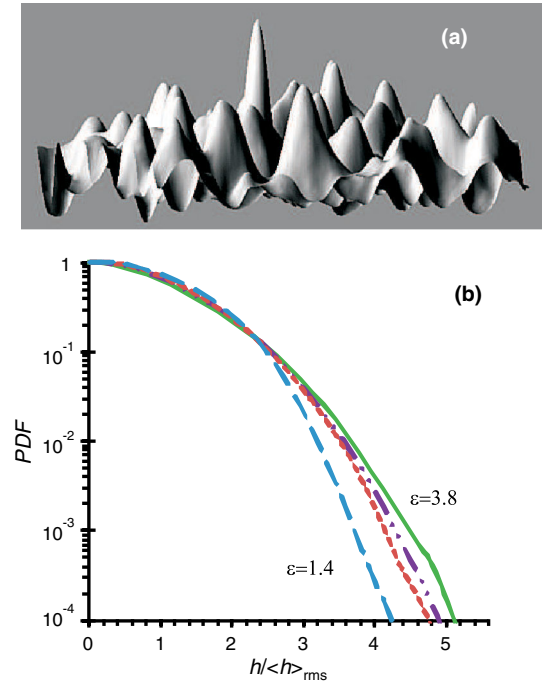


FIG. 4 (color online). (a) A snapshot of the surface ripple at high vertical acceleration, $\epsilon = 3.8$, illustrating extreme wave event. (b) Probability density functions of the positive surface elevations for different drives, $\epsilon = 1.4, 2.4, 2.9, 3.8$.

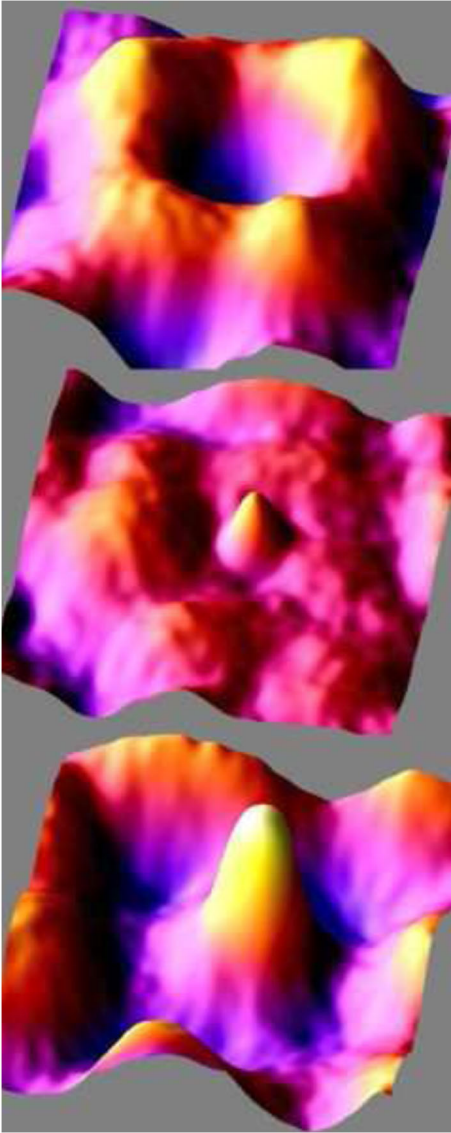


FIG. 5 (color online). Development of a rogue wave. Frames are taken at (top to bottom) t_0 , $t_0 + T/6$, $t_0 + T/2$, where T is the period of the oscillon pulsation (30 Hz).

a ridge whose amplitude is not higher than amplitudes of oscillons before the merger, as can be seen in Fig. 1(b).

The development of a rogue wave is however a collective effect due to the oscillon interaction. This is illustrated in Fig. 5. The formation of a rogue wave is preceded by a merger of 4 to 5 oscillons forming a deep crater, as seen in Fig. 5, top image. The rogue wave then emerges from the center of that crater. The rate of the crater formations increases with the increase in the oscillon merger rate due to increased mobility at higher drives.

It should be noted that, as has been previously reported, very small additions of organic polymers to water lead to a dramatic reduction in the oscillon mobility and to the narrowing of the frequency spectra [13]. In the reported experiments small additions of milk to water also reduce

spectral width. However even smaller concentrations of added surfactant render the effects of polymers negligible and restore the spectral width and mobility back to the levels observed in distilled water. This has been tested while measuring the frequency spectra using laser light reflected off the liquid surface, as described in [15].

Summarizing, Faraday ripples on the water surface consist of bound oscillons which form lattices. An increase in the vertical acceleration brings up horizontal drift of oscillons and leads to the breaking of the lattice order, faster motion of oscillons, and to their merger. Simultaneously, a strong increase in the probability of very high wave events, or rogue waves is observed. The generation of rogue waves is preceded by the formation of deep craters which result from the oscillon mergers. The horizontal mobility of oscillons and their merger seem to be the key processes in the rogue wave generation. What remains unclear is the mechanism driving horizontal motion of oscillons. There are indications that standing oscillons emit propagating waves, as illustrated in Fig. 3 of Ref. [13]. A spectrum of such waves consists of discrete frequency harmonics seen in Fig. 2(a). It is possible that the oscillon interaction occurs via wave emission, as has been recently proposed in [26].

This work was supported by the Australian Research Council's Discovery Projects funding scheme (DP110101525). Part of the analysis was performed while HX and MS attended the *New Directions in Turbulence* program at the Kavli Institute for Theoretical Physics China (KITPC) supported by the Project of Knowledge Innovation Program (PKIP) of Chinese Academy of Sciences, Grant No. KJCX2.YW.W10.

*Hua.Xia@anu.edu.au

†ICFP, Département de Physique de l'École Normale Supérieure, 24 rue Lhomond, 75005 Paris, France.

- [1] A. Kudrolli and J.P. Gollub, *Physica (Amsterdam)* **97D**, 133 (1996).
- [2] D.I. Goldman, M.D. Shattuck, Sung Joon Moon, J.B. Swift, and H.L. Swinney, *Phys. Rev. Lett.* **90**, 104302 (2003).
- [3] A. V. Kityk, J. Embs, V. V. Mekhonoshin, and C. Wagner, *Phys. Rev. E* **72**, 036209 (2005).
- [4] I. Shani, G. Cohen, and J. Fineberg, *Phys. Rev. Lett.* **104**, 184507 (2010).
- [5] A. von Kameke, F. Huhn, G. Fernandez-Garcia, A.P. Munuzuri, and V. Perez-Munuzuri, *Phys. Rev. Lett.* **107**, 074502 (2011).
- [6] W.B. Wright, R. Budakian, and S.J. Putterman, *Phys. Rev. Lett.* **76**, 4528 (1996).
- [7] D. Snouck, M.-T. Westra, and W. van de Water, *Phys. Fluids* **21**, 025102 (2009).
- [8] E. Falcon, *Discrete Contin. Dyn. Syst.* **13**, 819 (2010).
- [9] J. Wu, R. Keolian, and I. Rudnick, *Phys. Rev. Lett.* **52**, 1421 (1984).
- [10] O. Lioubashevski, H. Arbell, and J. Fineberg, *Phys. Rev. Lett.* **76**, 3959 (1996).

- [11] H. Xia, M. Shats, and H. Punzmann, *Europhys. Lett.* **91**, 14002 (2010).
- [12] J. Rajchenbach, A. Leroux, and D. Clamond, *Phys. Rev. Lett.* **107**, 024502 (2011).
- [13] M. Shats, H. Xia, and H. Punzmann, *Phys. Rev. Lett.* **108**, 034502 (2012).
- [14] Y. Couder, S. Protiere, E. Fort, and A. Boudaoud, *Nature (London)* **437**, 208 (2005).
- [15] M. Shats, H. Punzmann, and H. Xia, *Phys. Rev. Lett.* **104**, 104503 (2010).
- [16] M. Faraday, *Philos. Trans. R. Soc. London* **121**, 299 (1831).
- [17] P. B. Umbanhowar, F. Melo, and H. L. Swinney, *Nature (London)* **382**, 793 (1996).
- [18] H. Punzmann, M. G. Shats, and H. Xia, *Phys. Rev. Lett.* **103**, 064502 (2009).
- [19] P. J. Cobelli, A. Maurel, V. Pagneux, and P. Petitjeans, *Exp. Fluids* **46**, 1037 (2009).
- [20] F. Moysi, M. Rabaud, and K. Salsac, *Exp. Fluids* **46**, 1021 (2009).
- [21] W. B. Wright, R. Budakian, D. J. Pine, and S. J. Putterman, *Science* **278**, 1609 (1997).
- [22] A. V. Kityk, K. Knorr, H.-W. Muller, and C. Wagner, *Europhys. Lett.*, **65**, 857 (2004).
- [23] M. D. Abramoff, P. J. Magalhaes, and S. J. Ram, *Biophotonics International* **11**, 36 (2004).
- [24] J. C. Crocker and D. G. Grier, *J. Colloid Interface Sci.* **179**, 298 (1996).
- [25] N. B. Tufillaro, R. Ramshankar, and J. P. Gollub, *Phys. Rev. Lett.* **62**, 422 (1989).
- [26] D. Turaev, A. G. Vladimirov, and S. Zelik, *Phys. Rev. Lett.* **108**, 263906 (2012).